Spontaneous Emergence of Long-range Shape Symmetry

Hidetsugu Shiozawa,[*,†] Anne C. Skeldon,[‡] David J. B. Lloyd,[‡] Vlad Stolojan,[†]

David C. Cox,[†] and S. Ravi P. Silva[*,†]

Advanced Technology Institute, University of Surrey, Guildford, GU2 7XH, United Kingdom, and

Department of Mathematics, University of Surrey, Guildford, GU2 7XH, United Kingdom

E-mail: h.shiozawa@surrey.ac.uk; s.silva@surrey.ac.uk

Abstract

Self-organisation of matter is essential for natural pattern formation, chemical synthesis, as well as modern material science. Here we show that iso-volumetric reactions of a single organometallic precursor allow symmetry breaking events from iron nuclei to the creation of different symmetric carbon structures; micro-spheres, nanotubes, and mirrored spiralling micro-cones. A mathematical model, based on mass conservation and chemical composition, quantitatively explains the shape growth. The genesis of such could have significant implications for material design.

Keywords Synthesis, Carbon nano- and micro- structure, Modelling of synthetic process

[*]To whom correspondence should be addressed

[†]Advanced Technology Institute, University of Surrey, Guildford, GU2 7XH, United Kingdom

[‡]Department of Mathematics, University of Surrey, Guildford, GU2 7XH, United Kingdom

Symmetry is central to the design of nature and has intrigued humanity over centuries. Society has embraced symmetry, knowingly and unknowingly, in everyday life as well as their own genetic blueprint which stems from the original work to unravel the structure of DNA.[1] At subatomic levels, the cause of broken symmetry is the origin of a predominance of matter over antimatter in the Universe.[2] Chiral symmetry is fundamental to physical, chemical and biological functionality, seen for instance as optical activity[3] and chemical wave. Frequently, one chirality dominates; amino acids in proteins are almost exclusively left-handed, while most sugars in nucleic acids are right-handed. The majority of DNA in living cells have right-handed double helical structures.[1] Morphological manifestations of left-right asymmetry are seen at all scales, for example in the placement of organs of animal and the helicity of shell spiral.[4] Mechanisms governing the natural growth of symmetric patterns have long intrigued scientists and remain central to modern science from attempts to understand the spiralling of natural filamentary materials (tendrils of climbing plants[5]) to DNA[1] and the studies of bacterial macrofibers.[6] Self-assembly of atoms and molecules is the key to understanding the natural shape formation as well as synthesis of new materials, including single crystals (silicon, synthetic diamond[7]), synthetic polymers (e.g. Bakelite, nylon), and nanostructured carbon (carbon fiber, fullerene,[8] carbon nanotube[9]). Helical structures are seen in polymers,[10] carbides,[11] oxides[12–14] and carbons.[15,16] All these synthesis techniques, in essence, allow the transformation of liberated precursor atoms and molecules into mesoscopic structures of higher symmetry.

Here we demonstrate the self-pressured synthesis using an iso-volumetric process from a pure organometallic precursor and show that novel micro-graphitic structures of high symmetry can be created. Three types of symmetric structure are spontaneously generated via the same experimental process but for different ranges of temperature and vapour pressure, allowing a phase diagram of the different structures to be produced. The structures are classified by differing types of symmetry; spherical (micro-particles), cylindrical (carbon nanotubes) and reflectional symmetry (mirrored micro-cones). In particular, the micro-cones undergo spiralling where, unlike traditional carbon materials, symmetric arms of opposite chirality are created.

All the structures are produced by a constant-volume process using ferrocene as a single precursor. In each case, the ferrocene is vacuum-sealed in a glass ampule and then heated in a furnace. From the initial quantity of the ferrocene and the volume of the ampule, the effective pressure of ferrocene is determined at a given temperature (see supporting information for further details). At temperatures higher than $\sim 590\,^{\circ}$C, the ferrocene dissociates and spontaneously forms into different structures, as summarised in Figure 1. For effective pressures of ferrocene below 5 MPa and temperatures between 590 – 650°C, spherical particles are formed; for similar pressures but higher temperatures, carbon nanotubes are observed (Figure 1c). It is at effective pressures that exceed 5 MPa that our novel spiralling structures are synthesised in high purity and large yield (Figure 1d-h and the supporting figure: Figure S1). The novel structures have two 'arms' that emerge from an approximately spherical core. There is a very high degree of reflectional symmetry between each arm, with each twist and each imperfection in one arm mirrored by a similar twist or imperfection in the other. For example, in Figure 1h the helicity reverses direction at the same point on both sides (see the points indicated by arrows in Figure 1h). The bright spherical area observed at the centre of the structures is found to be an iron-rich core whereas the arms are almost pure solid graphitic carbon; see Figure 2 where we show the electron microscopy images of a cross-section of a micro-spiral near the centre. Electron diffraction images in Panel d show the graphitic layers spiralling out from the central carbide core.

In all three cases the symmetry of shape emerges spontaneously in a template-free process. In the case of the spiralling arms, the presence of the high degree of reflectional shape symmetry on the scale of several tens of micrometers suggests that these structures do not grow from a vapour deposition process, but grow out symmetrically from a central 'seed' core. Each of the three states that is formed can be understood as occurring as result of a similar process that initiates with the dissociation of the ferrocene to produce a vapour that then forms 'seeds' due to local density variations. Due to the almost isotropic nature of the vapour, these seeds will have O(3) (spherical) symmetry. If the growth is sufficiently slow, as in the case of the lower temperatures and pressures in our experiments, then the spherical symmetry of the seeds is preserved and the micro-spheres

shown in Figure 1b are produced. For faster growth rates, as occurring at higher temperatures and/or pressures, this spherical growth becomes unstable and we expect symmetry breaking to occur.

For problems with symmetry breaking, symmetric bifurcation theory has proved a powerful tool that enables the identification of the kind of patterns that are to be expected when a transition from a symmetric state occurs (see supporting information).[17] Generically, if a highly symmetric state becomes unstable, it will do so only by losing some of its symmetry. The value of this technique is that it can deduce behavioural changes from the symmetry of a state alone. In the case of a state with O(3) symmetry, the different possible states can be represented by the spherical harmonics, $Y_l^m(\theta, \varphi)$.[18] Both the nanotubes and the mirrored cones can be understood as occurring as a result of transitions from an O(3) symmetric state $(l = 0)$ to a state when carbon is unevenly distributed on the surface of the sphere, resulting in the growth of nanotubes ($l = 1$) and mirrored micro-cones ($l = 2$). In Figure 1, the three spherical harmonics $l = 0, 1$ and $l = 2$ are shown. The colour of the sphere corresponds to the value of spherical harmonics and, in our case, the red area points to the direction in which the micro structure is formed, while elemental sources are supplied through the blue area.

In the region where helical micro-structures are found, many different individual examples are observed, each at a different stage of growth—statistical fluctuations mean that they do not start to grow at exactly the same point in time. Since the process has to stop once all the iron and carbon from the ferrocence has been used, some structures reach a more advanced stage than others. The spiraling occurs when the diameter of the arms is small (see Figure 1f-h). As the arms grow further the shape becomes straighter, as seen in Figure 1e. From observations of different examples we find a correlation between the diameter of the core and the length of the structures, see Figure 3a, suggesting that the core and the cone grow at the same time. By making the assumptions that the core and carbon arms grow simultaneously so that at any point in time the radius of the arms is the same as the radius of the core; the arms grow by the continuous extrusion of graphitic disks (due to bulk-diffusion), the number of atoms accumulates on the core and each arm at constant rates k_C

and k_A, respectively, then conservation of mass leads to the relation

$$L_{th} = \frac{v_A}{v_C}\frac{k_A}{k_C}D,$$

where L_{th} is the length of the cones and D is the diameter of the core (see the supporting information for further details). This predicts that the length of the cone is linearly related to the diameter of the core with a cone angle θ given by

$$\theta_{th} = 2\arctan\left(\frac{1}{2}\frac{v_C}{v_A}\frac{k_C}{k_A}\right).$$

Since ferrocene is $Fe(C_5H_5)_2$ and electron diffraction measurements of the core suggest that it is predominantly cementite (Fe_3C) we take $k_A/k_C = 29/1$. Using v_A = 5.29 cm^3/mol and v_C = 22.83 cm^3/mol for the molar volumes of graphitic arms and iron-carbide core, respectively, our model predicts $L_{th} = 6.7D$ and that the cone angle is $\theta_{th} = 0.15$ radians. The model predictions are compared with the experimental results in Figure 3a and Figure 3b.

In Figure 3a, the linear relationship between the length of the microstructures and the diameter, as predicted by the model is clearly shown. The best fit line, $L = (4.3 \pm 0.3)D + (1.1 \pm 0.8)$, passes close to the origin, consistent with the model prediction. The experimental lengths are found to be on average 75 % of the theoretical values for the same diameter. The experimental lengths are necessarily shorter than the length predicted by the mathematical model because the length measurement does not take into account the spiralling of the tips of the cone—the mathematical cone length should be regarded as providing an upper bound rather than a best fit to the experimental data.

In Figure 3b, the angle of the cone is well approximated by the model with an experimental angle $\theta = 0.18 \pm 0.04$ radians. There is a small increase in the cone angle as the diameter increases. A possible cause of this could be that the concentration of carbon in the core varies with the core size. It is known that the solubility of carbon in metal reduces when the volume of metal becomes nanoscale[19] and the observed small increase in the cone angle is consistent with a small increase of

carbon concentration in the core as the iron core grows from nano to micro scale. A change in the concentration of carbon in the core could be incorporated in the mathematical model by allowing the ratio $v_C k_C / v_A k_A$ to depend on the diameter of the core. Our assumption in the mathematical model that the core was made of pure cementite is based on the STEM-diffraction observations (Figure 2d). However, the energy filtered TEM image (Figure 2c) does show that there are carbon rich domains within the core. The difference between the mathematical calculation of the angle, $\theta_{th} = 0.15$ radians, and the experimental measurement, $\theta = 0.18 \pm 0.04$ could be accounted for if the core was composed of 84% cementite and 16% carbon by volume.

The spiralling of the conical arms is intriguing and is a signature for the symmetry of growth. One explanation for this is that the axi-symmetric core state that generates the two arms is time-dependent, causing the distribution of carbon on the surface of the core to rotate against the existent cones. Since the arms grow from the core, a rotating distribution of carbon at the core around the symmetry axis would lead to the helical symmetry of opposite handedness. The flip-flop of the chirality, as seen in Figure 1h, is explained as a consequence of the reverse of the course of rotation at one time. This picture is consistent with the electron diffraction images taken at the positions marked with open circles in Figure 2d that show the angle of the graphite c-axis rotates continuously as it goes around the core. The graphitic layers grow tangentially in the vicinity of the iron core. This is in-line with the presence of the rotational motion of the growth activity against the cone arms. Note that this dictates that the two arms need to have opposite chirality; the rotation about the axis has to be in the same direction in both hemispheres otherwise a singularity in the flow of carbon would occur at the equator.

We have studied the spontaneous formation of nano/micro structures of different symmetry arising from the self-pressured synthesis from a single organometallic precursor. Based solely on mass conservation and the chemical composition, a mathematical model is created that provides quantitative agreement with the experiment with no parameter fitting. Good agreement between the theory and experiment on the cone shape supports our hypothesis for the symmetric growth process. The high levels of symmetry and purity of the formed micro- and nano- structures suggest

that exploiting such a self-organisation process can provide an advance in current state-of-the-art technologies with regard to morphological complexity and selectivity. Key technological advances to the state-of-the-art in complex structure design and synthesis could be provided by this research which exploit a self-pressured catalytic process. The study also provides insight into the rules that govern natural pattern formations, and that potentially govern future technology.

Acknowledgement

H. S. acknowledges the Leverhulme Trust for support through an early career fellowship. S. R. P. Silva thanks the EPSRC for financial support through a Portfolio Partnership award. We thank J. Underwood, C. Buxey, D. Mansfield, T. Corless and M. Blissett for technical assistance.

References

(1) Watson, J. D.; Crick, F. H. C. *Nature* **1953**, *171*, 737–738.

(2) Nambu, Y.; Jona-Lasinio, G. *Phys. Rev.* **1961**, *122*, 345–358.

(3) Pasteur, L. *Ann. Chim. Phys.* **1848**, *24*, 442–459.

(4) Patel, N. H. *Nature* **2009**, *462*, 727–728.

(5) Darwin, C. R. *The Power of Movement in Plants*; John Murray, London, 1880.

(6) Goldstein, R. E.; Goriely, A.; Huber, G.; Wolgemuth, C. W. *Phys. Rev. Lett.* **2000**, *84*, 1631–1634.

(7) Bundy, F. P.; Hall, H. T.; Strong, H. M.; Wentorf, R. H. *Nature* **1955**, *176*, 51–55.

(8) Kroto, H. W.; Heath, J. R.; O'Brien, S. C.; Curl, R. F.; Smalley, R. E. *Nature* **1985**, *318*, 162–163.

(9) Iijima, S. *Nature* **1991**, *354*, 56–58.

(10) Frette, V.; Tsafrir, I.; Guedeau-Boudeville, M.; Jullien, L.; Kandel, D.; Stavans, J. *Phys. Rev. Lett.* **1999**, *83*, 2465–2468.

(11) Zhang, H.; Wang, C.; Wang, L. *Nano Lett.* **2002**, *2*, 941–944.

(12) Zhang, H.; Wang, C.; Buck, E. C.; Wang, L. *Nano Lett.* **2003**, *3*, 577–580.

(13) Kong, X. Y.; Ding, Y.; Yang, R.; Wang, Z. L. *Science* **2004**, *303*, 1348–1351.

(14) Gao, P. X.; Ding, Y.; Mai, W.; Hughes, W. L.; Lao, C.; Wang, Z. L. *Science* **2005**, *309*, 1700–1704.

(15) Baker, R. T. K.; Harris, P. S.; Terry, S. *Nature* **1975**, *253*, 37–39.

(16) Amelinckx, S.; Zhang, X. B.; Bernaerts, D.; F., Z. X.; Ivanov, V.; Nagy, J. B. *Science* **1994**, *265*, 635–639.

(17) Golubitsky, M.; Stewart, I.; Schaeffer, D. G. *Singularities and groups in bifurcation theory. Vol. II*; Applied Mathematical Sciences; Springer-Verlag: New York, 1988; Vol. 69; pp xvi+533.

(18) Matthews, P. C. *Nonlinearity* **2003**, *16*, 1449–1471.

(19) Harutyunyan, A. R.; Awasthi, N.; Jiang, A.; Setyawan, W.; Mora, E.; Tokune, T.; Bolton, K.; Curtarolo, S. *Phys. Rev. Lett.* **2008**, *100*, 195502.

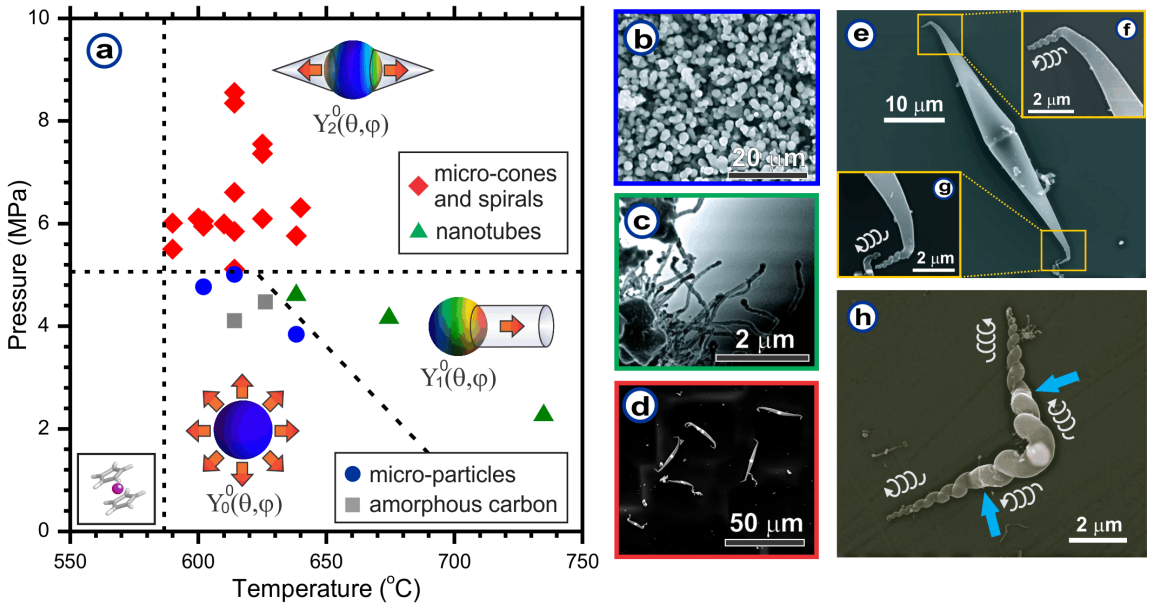

Figure 1: **a**, Phase diagram for spiralling micro-cones, nanotubes and micro-particles. For effective pressures above 5 MPa and temperatures above 590 °C, we observe mirrored micro-cones and spirals. The schematics show the carbon structures growing out from the spherical core into the directions indicated by arrows. The colour of the sphere represents the value of the spherical harmonics that identify the growth symmetry. The bottom-left inset shows the molecular structure of ferrocene, an iron atom sandwiched between two C_5H_5 rings. Scanning Electron Microscope (SEM) images for the various structures are shown in **b**-**h**. **b**, micro-particles, **c**, nanotubes, **d** shows micro-cones and spirals. **e**, a micro-cone with zoom-in of the spiralling tips in panels **f** and **g**. **h**, a micro-spiral highlighting the fact that the spiralling arms are of opposite chirality.

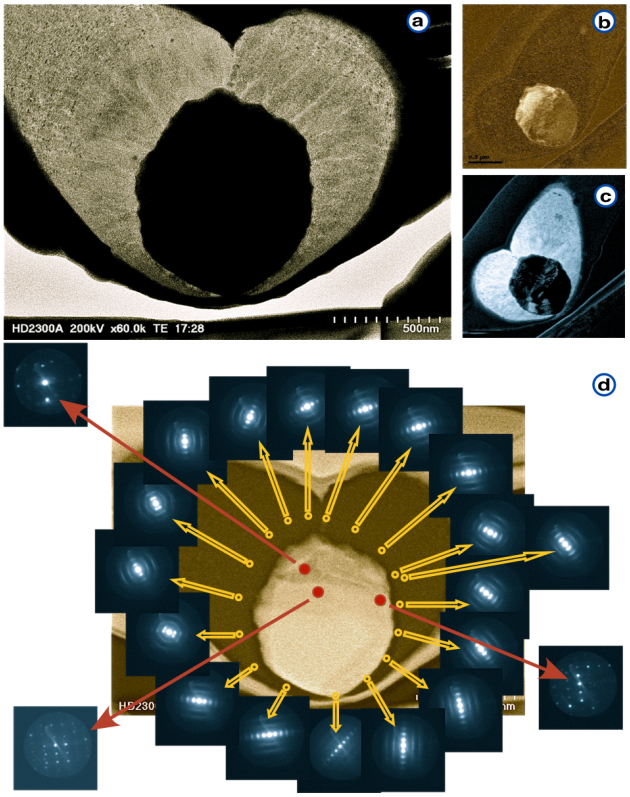

Figure 2: **a**, Scanning Transmission Electron Microscope (STEM) bright-field image for the cross-section cut through the core (dark sphere) as well as the two cones (brighter areas), using a Focussed Ion Beam (FIB) microscope. The dark region on the outside is a tungsten layer that protects the sample during the FIB sectioning. **b**, Energy-filtered TEM images of the distribution of iron, showing the centre is predominantly iron rich. **c**, The equivalent EFTEM carbon map shows that the arms of the micro-cone are carbon rich and that the metallic core also contains carbon-rich phases. **d**, electron diffraction images superimposed on a Z-contrast STEM image, collected at the position indicated by arrows, showing that the c-axis of the graphitic layers continuously rotates around the core.

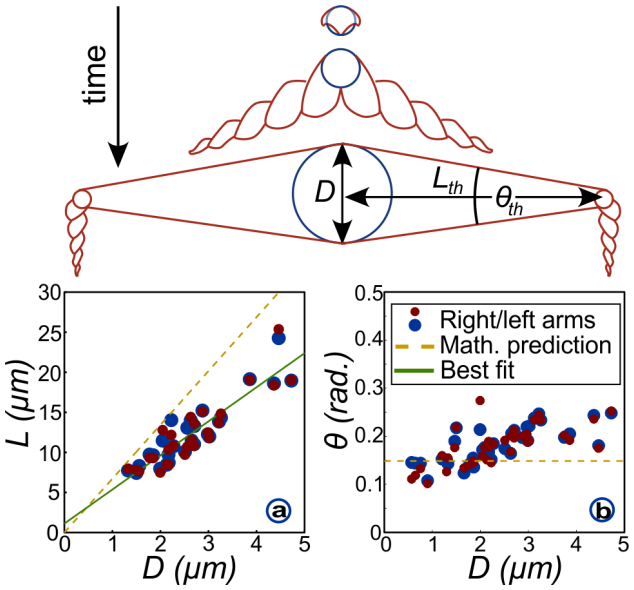

Figure 3: The mathematical model for the growth of the micro-cones is shown from which the length of the cones is predicted to be $L_{th} \approx 6.7D$ (shown in **a**) and the angle of the cone $\theta_{th} \approx 0.15$ radians (shown in **b**). Experimentally, the length of the cones is found to be $L = (4.3 \pm 0.3)D + (1.1 \pm 0.8)$ and the cone angle to be $\theta = 0.18 \pm 0.04$ radians. Differences between left and right arms is $\approx 4.2\%$ in average for L and $\approx 6.6\%$ for θ and within experimental error. (Right and left arm is an arbitrary designation).